Drives and fates of plastic pollution forming anthropogenic stones in beach environments

ABSTRACT

Plastic litter can remain permanently on record strata when it occurs as anthropogenic stones due to their susceptibility to burial processes. To verify this phenomenon, we monitored in-situ plastistone between 2019 and 2024 on the most remote island where they have been reported so far. Plasticlasts formed by the weathering of in-situ plastistone were transported by currents and deposited along Trindade Island's shorelines. Plasticlasts were also buried in green turtle nests at a large South Atlantic Ocean nesting hotspot. The turtle nest morphology act as local sedimentary traps facilitating the accumulation and burial of them. Our study provides first plasticlast morphometric analysis to track their dispersion through time reveling history of transport and reworking by surface processes. We proposed a new baseline for anthropogenic stones using portable Raman spectroscopy. We determined the polymer type in the melted matrix and detected dye additives, both crucial for tracing the sources of the plastic items burned to form them. Our results show that maritime ropes, mainly composed of polyethylene with phthalocyanine dye, were the primary source of plastistone composition on Trindade Island. Such pollution from shipping and maritime activities likely resists melting, transport, and deposition processes until final burial. Our study reveals a concerning trend how anthropogenic stones are increasingly becoming integral to marine depositional processes and permeate marine ecosystems.

Key-words: Anthropocene; plasticlast; plastic debris; maritime ropes; environmental monitoring; Raman.

Preprint not peer reviewed

This preprint research paper has not been peer reviewed. Electronic copy available at: https://ssrn.com/abstract=5372354

1. INTRODUCTION

Human activity and plastic debris on beaches are forming anthropogenic stones highlighting the concerning incorporation of marine litter into Earth's surface dynamics (e.g., Corcoran et al., 2014; Fernandino et al., 2020; Santos et al., 2022; Rangel-Buitrago and Neal, 2023; Fernandino et al., 2025). Such emerging plastic pollutants provide crucial evidence of the Anthropocene due to their higher tendency to burial processes (Corcoran et al., 2014; Zalasiewicz et al., 2014).

Anthropogenic stones were first reported on an insular beach and described as a mudstone-siltstone-sandstone conglomerate within a matrix of melted plastic named plastiglomerate (Corcoran et al., 2014; Corcoran and Jazvac et al., 2020). However, plastic debris forms also occur as homogenous plastic matrix with no sediment incorporate named plastistone that can be fragmented by weathering agents into plasticlasts (Santos et al., 2022). These novel plastic forms reported worldwide (e.g., Shruti et al., 2023) have integrated the geosphere and overwhelmed global ecosystems (Rangel-Buitrago et al., 2023).

To test the hypothesis that anthropogenic stones are likely to be buried, we monitored in-situ plastistone on an oceanic beach foreshore (Trindade Island, Brazil) during five years. We detected formation and transportation of plasticlasts that were deposited on the shoreline of other beaches and buried preferentially in green turtle nests. We outline the first baseline for analyzing anthropogenic stones using Raman spectroscopy. We provide detailed band assignments and vibrational models, which are crucial for understanding the geochemical signature of their melted plastic matrix. We also detected dye additives, for the first time, which is crucial to track plastic items sources. In this sense, pollution from shipping and maritime activities are the primary source of plastistone in the study area.

Preprint not peer reviewed

This preprint research paper has not been peer reviewed. Electronic copy available at: https://ssrn.com/abstract=5372354

2. MATERIALS AND METHODS

This study was carried out on remote Trindade Island in the South Atlantic Ocean, which is an offshore Brazilian territory located ca. 1,400 km from the mainland that hosts only military and scientific installations (Santos et al., 2022) (Figure 1). We monitored in-situ plastistone from 2019 to 2024 through field measurements, photographs, sample collection, and Raman characterization. Plasticlasts were also monitored and collected during this period, mainly at Turtle Beach, where the highest concentration was found.

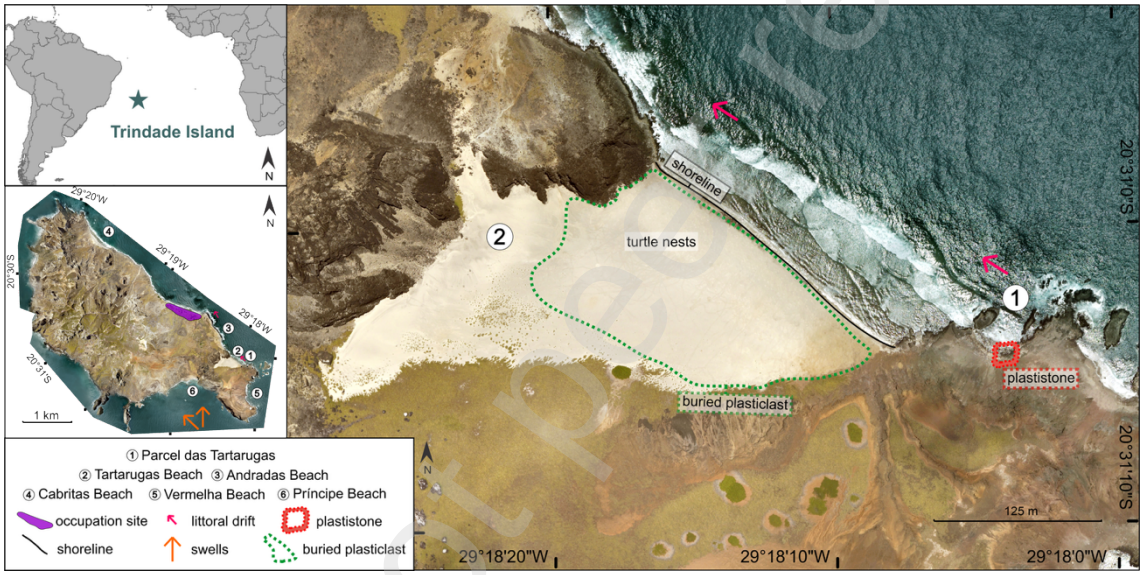


Figure 1: Study area: In-situ plastistone at (1) Parcel das Tartarugas (red dotted line), where erosion has been documented since 2019. Derived plastics were transported by currents to beaches (2)–(6), with Tartarugas Beach (2) accumulating along the shoreline (black line) and being buried in green turtle nests (green dotted line). Coastal-drift vectors (orange and pink arrow) are adapted from Angulo et al. (2018).

For lab analysis, 50 samples were cleaned and dried samples were then photographed. Magnified 200x images were obtained using the Zeiss SteREO Discovery.V12 stereomicroscope. Samples color was visually assessed, and mass was measured using a Shimadzu AUW220D analytical balance. Plasticlast shapes were

Preprint not peer reviewed

This preprint research paper has not been peer reviewed. Electronic copy available at: https://ssrn.com/abstract=5372354

66 classified using the Zingg (1935) method, based on the ratios of their long, intermediate,
67 and short axes measured with a digital caliper. Grain roundness was visually assessed
68 using the classification system of Pettijohn et al. (1987). Morphometric analyses to
69 quantify roundness, circularity, and aspect ratio were conducted with ImageJ software
70 (version 1.54k for Windows). Plasticlast density was determined by testing buoyancy in
71 tap water (e.g., Turner et al., 2019) at room temperature (approximately 22 °C) in
72 graduated glass beakers.

73 We applied Raman spectroscopy (e.g., Goswami and Bhadury, 2022) to
74 characterize the homogeneous melted plastic matrix, focusing on its elemental
75 composition and associated additives. However, micro-Raman analyses (Renishaw
76 inVia; 514, 633, and 785 nm excitation wavelengths) of the plastistone's melted-plastic
77 matrix failed to generate satisfactory spectra. We then used a Bruker portable Raman
78 spectrometer Bravo model, equipped with DuoLaserTM excitation (785 nm and 852 nm).
79 The laser power was 30 mW for both excitation wavelengths. During the analysis, it
80 automatically adjusts parameters such as laser power, acquisition time, and the number
81 of accumulations needed to optimize the signal-to-noise ratio. Analysis was conducted
82 on the surface and interior regions of each sample, as chemical treatment was not
83 required.

84 Raman band assignments were established by direct comparison with
85 authoritative polymer reference spectra. In this sense, the vibrational modes evaluated,
86 such as C–C skeletal stretches, CH_2 wagging and twisting, symmetric and asymmetric
87 CH_2 stretches, and their overtones, were matched to the assignments reported by Wool et
88 al. (1986), Pigeon et al. (1991), Sato et al. (2002a, 2002b), and Silva and Wiebeck (2019).
89 Polymer identity was further corroborated through spectral correlation with the Open
90 Specy library (Cowger et al., 2021).

Preprint not peer reviewed

This preprint research paper has not been peer reviewed. Electronic copy available at: https://ssrn.com/abstract=5372354

For dye additive analysis, Raman spectra were obtained from standard dye samples, which served as comparison standards, including Copper Phthalocyanine (CuPc; Sigma-Aldrich), Copper (II) Phthalocyanine Tetrasulfonic (CuTsPc; Sigma-Aldrich), Iron Phthalocyanine (FePc; Kodak), Nickel Phthalocyanine (NiPc; Kodak), Nickel (II) Phthalocyanine Tetrasulfonic (NiTsPc; Sigma-Aldrich), and Zinc Phthalocyanine (ZnPc; Kodak). The resulting spectra were analyzed by comparison with studies available to identify dyes, including Bratashov et al. (2011), Del Caño et al. (2003), Gaffo et al. (2002a), Gaffo et al. (2002b), Gaffo et al. (2004), Scherrer et al. (2009), and Zucolotto et al. (2003).

3. RESULTS

The spectrum obtained for in-situ (i.e., fixed on the ground) plastistone samples (Figure 2a, b) displayed characteristic PE bands, with seven Raman-active modes identified in our results (Figure 2c). The peaks at 1063 cm^{-1} and 1129 cm^{-1} correspond to asymmetric and symmetric C–C stretching along the polymer backbone, respectively. The 1173 cm^{-1} feature reflects CH_2 wagging deformation, whereas twisting of CH_2 groups generates the 1295 cm^{-1} band, and an additional bending mode appears at 1418 cm^{-1}. A Fermi-resonant doublet at 1441 cm^{-1} and 1459 cm^{-1} arises from coupled CH_2 deformations and their overtones. At higher wavenumbers, the bands at 2849 and 2883 cm^{-1} correspond to the symmetric and asymmetric CH_2 stretching vibrations, respectively, whereas the weaker feature at 2725 cm^{-1} represents an overtone that completes the PE spectral profile.

Preprint not peer reviewed

This preprint research paper has not been peer reviewed. Electronic copy available at: https://ssrn.com/abstract=5372354

The polyethylene grade was distinguished by the relative intensities of the diagnostic band set at 1063, 1129, 1418, 1441, and 1459 cm^{-1}, which is characteristic of high-density polyethylene (HDPE), witch match with Open Specy library.

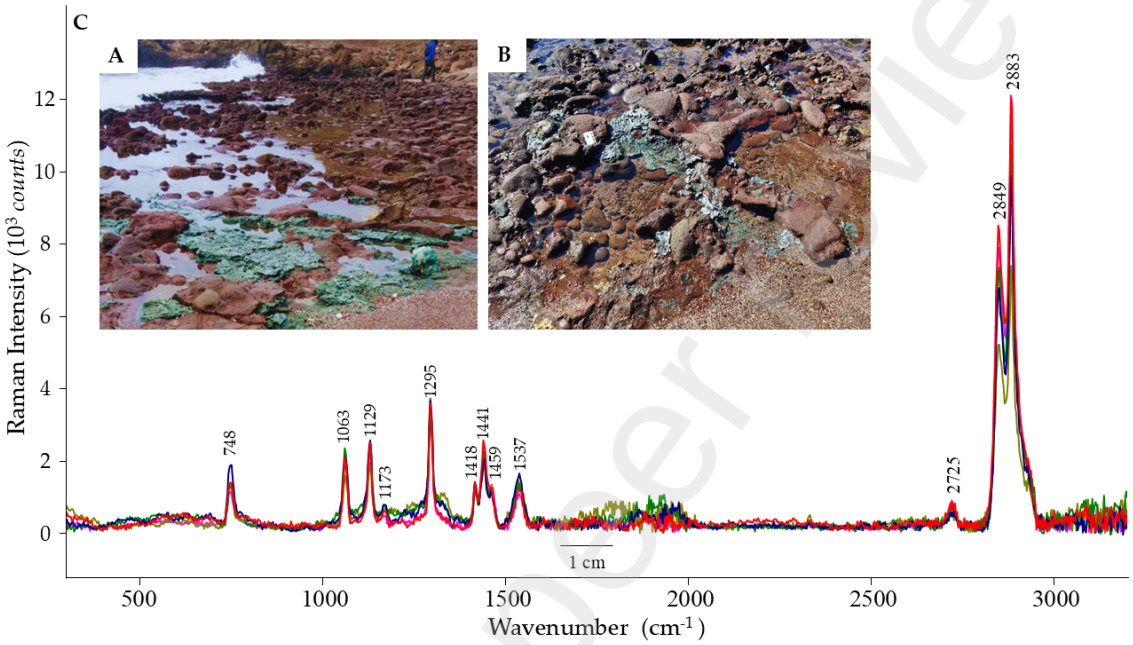


Figure 2: In-situ plastistone monitoring: A) Outcrop in 2019 (Santos et al., 2022) showed erosion of 45% until B) 2024, witch part of the outcrop was buried during the beach depositional season. Over five years, slight discoloration and C) minor variations in spectral peaks.

In addition to the PE bands, we observed two bands at 748 and 1537 cm-1 in the plastistone Raman spectrum (Figure 2), which are not PE characteristics. We observed that other metallic phthalocyanines (CuPc, CuTsPc, FePc, NiPc, NiTsPc, and ZnPc) also exhibit bands near 748 and 1537 cm^{-1} (Figure 3). Furthermore, we highlight CuTsPc, which has a band at 747 cm^{-1} and another at 1530 cm^{-1}, possibly indicating the pigment present in the plastistone. The intense band at 1530 cm^{-1} is attributed to (C=N) stretching of the pyrrole group and isodronil stretching. The band at 747 cm^{-1} is attribute to the macrocycle vibration, ring stretching, and the angular deformation (C-H wagging).

Preprint not peer reviewed

This preprint research paper has not been peer reviewed. Electronic copy available at: https://ssrn.com/abstract=5372354

The Raman bands attributed to different classes of copper phthalocyanines exhibit distinct spectral characteristics: chlorinated copper phthalocyanine in the alpha form shows bands at 747 and 1525 cm^{-1}, while non-chlorinated copper phthalocyanine exhibits bands at 748 and 1522 cm^{-1}, and its beta form shows bands at 747 and 1530 cm^{-1}. This band (Figure 3) matches the spectral characteristics of chlorinated copper phthalocyanine, which exhibits a band at 1538 cm^{-1}.

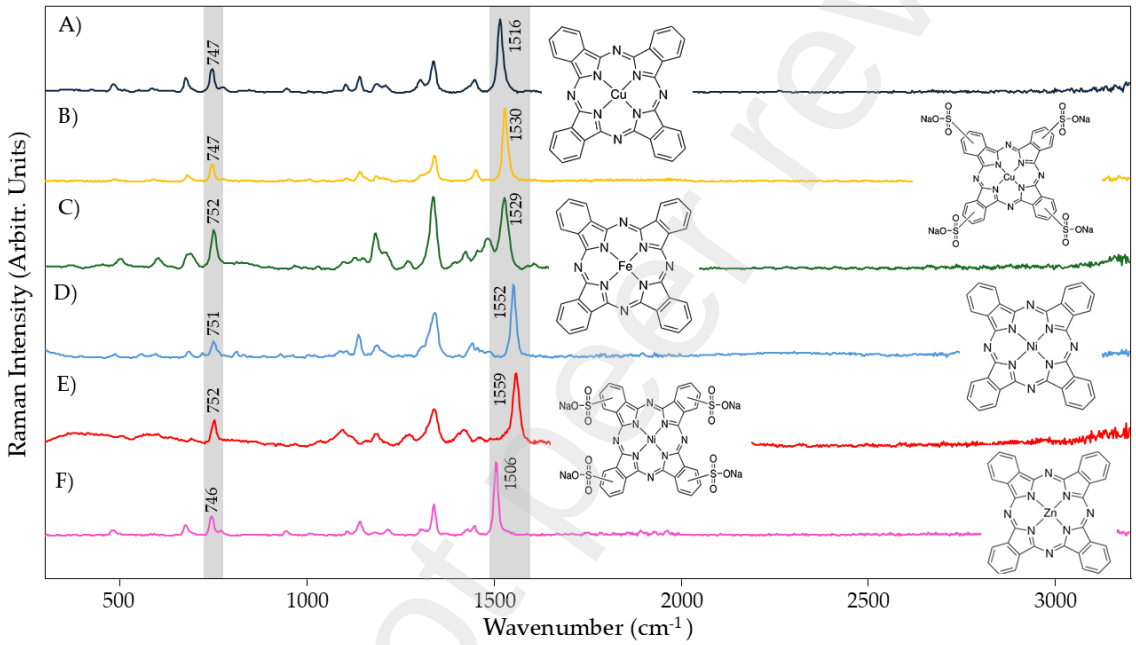


Figure 3: Raman spectra of phthalocyanine dyes in powder form: A) Copper phthalocyanine; B) Copper (II) phthalocyanine; C) Iron phthalocyanine; D) Nickel phthalocyanine; E) Nickel (II) phthalocyanine tetrasulfonic; and F) Zinc phthalocyanine.

Within these plastistone, we detected preserved green ropes (Figure 4). The Raman spectrum obtained from the fibers of the green ropes shows characteristic bands of high-density PE. However, the bands 685, 740, 783, 1214, 1540, and 2329 cm^{-1} do not correspond to PE. The evidence obtained in our analysis suggests that the dye identified in the plastistone and the preserved green rope corresponds to a phthalocyanine, as indicated by the presence of a band at 1537 cm^{-1}.

Preprint not peer reviewed

This preprint research paper has not been peer reviewed. Electronic copy available at: https://ssrn.com/abstract=5372354

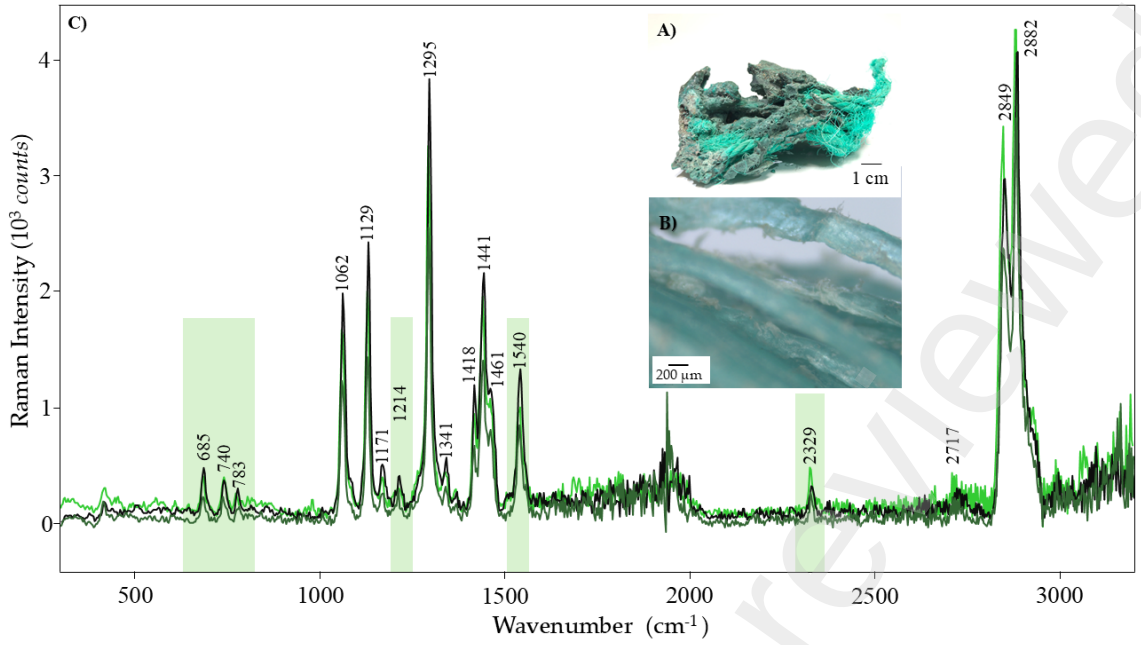


Figure 4: Maritime ropes as a source material in plastistone composition: A) Preserved green rope in plastistone; B) Microscopic image of rope fibers; and C) Raman spectra representing distinct regions of the preserved rope.

Plasticlasts from Parcel das Tartarugas`s plastistone were observed on Tartarugas, Vermelha, Andradas, Cabritos, and Principe beaches (Figure 1). However, we documented a concerning amount of deposition on Tartarugas Beach, ranging from a few meters to nearly 500 meters from the outcrop, where a large nesting ground of the green sea turtle (Chelonia mydas) is located (Figure 5). We analyzed 45 plasticlasts that exhibit a range of green and grey shades, varying in size from micro to macro, porosity from low to high, and displaying flow structures and polygonal fracturing patterns (Figure 6a).

Preprint not peer reviewed

This preprint research paper has not been peer reviewed. Electronic copy available at: https://ssrn.com/abstract=5372354

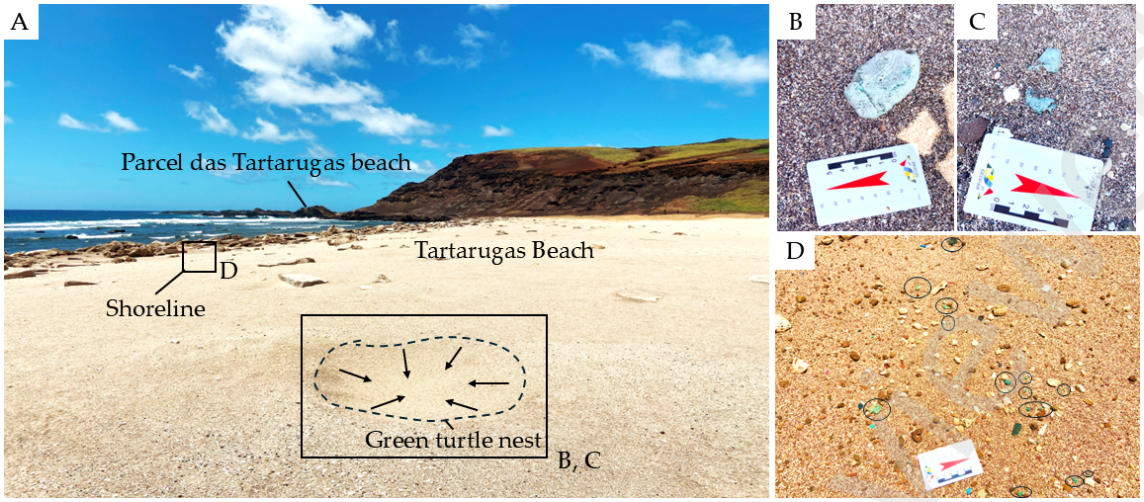


Figure 5: Plasticlasts deposition along Tartarugas Beach: A) Plasticlats were found along the shoreline and buried in turtle nests, including the distal end of the beach.; B) Samples were collected on the surface, C) undergoing burial, and D) several others were located along the beach, as indicated by black circles.

All plasticlasts collected (Figure 6a) have a density lower than that of freshwater (<1.0 g/cm³). Mass ranged from 68 mg to 4.234 g, with a median value of approximately 520 mg. All clast dimensions are strongly correlated with mass ($R^2 > 0.77$), with a slightly higher correlation for the intermediate axis, suggesting a subtle predominance of this dimension in influencing clast mass (Figure 6b). Long diameters ranged from 8.69 to 37.61 mm (median = 17.41 mm), intermediate diameters from 6.18 to 27.12 mm (median = 11.68 mm), and short diameters from 3.7 to 19.49 mm (median = 7.41 mm).

Morphological analysis of plasticlasts (Figure 6c, d) shows they are predominantly subrounded with low sphericity (25.6%), followed by subrounded with high sphericity (23.3%). Other notable categories include subrounded with moderate sphericity (14.0%) and subangular with high sphericity (14.0%). Smaller proportions were observed for subangular with moderate (7.0%) and low sphericity (4.7%), as well as rounded with high sphericity (4.7%). Less common types, each representing 2.3%, include angular particles with high or low sphericity, and rounded with moderate

Preprint not peer reviewed

This preprint research paper has not been peer reviewed. Electronic copy available at: https://ssrn.com/abstract=5372354

sphericity. ImageJ measurements showed sample circumferences ranged from 0.56 to 0.829 (median = 0.728; mean = 0.718; SD = 0.065), while roundness ranged from 0.429 to 0.971 (median = 0.730; mean = 0.723; SD = 0.134). Among the 43 samples, prolate particles were most frequent (34.9%), followed by oblate (30.2%), equant (23.3%), and bladed shapes (11.6%).

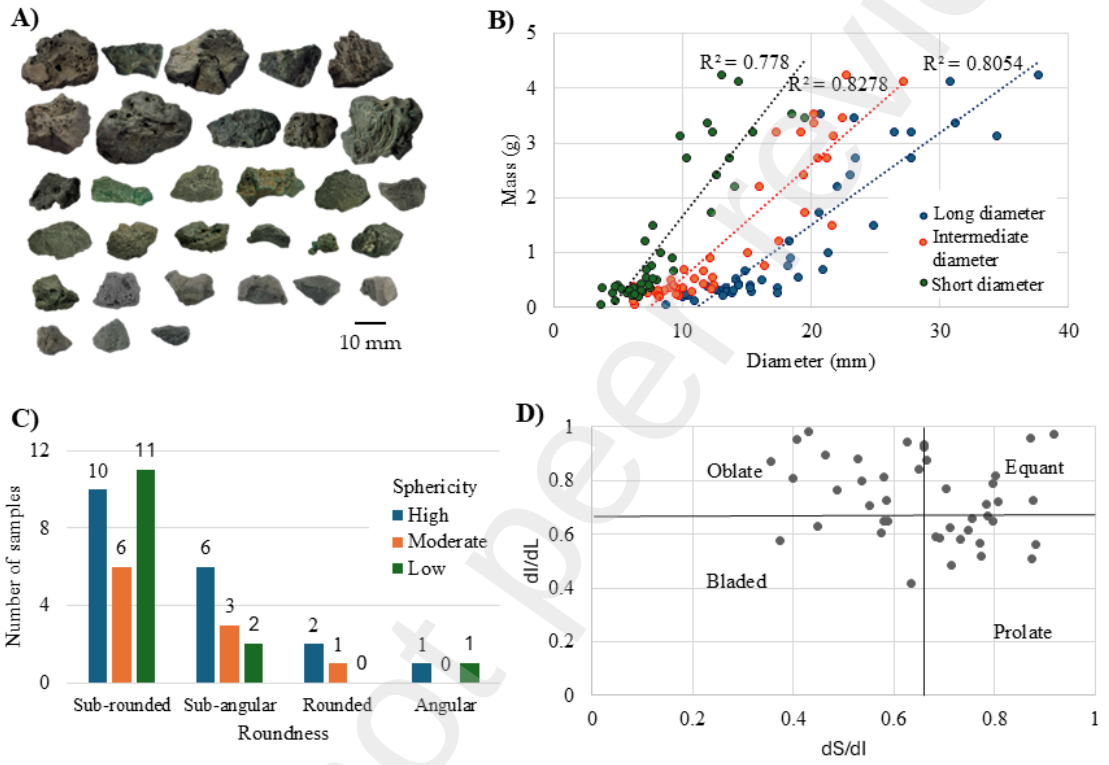


Figure 6: Morphometric correlations: A) Plasticlast transported in a beach environment; B) Scatter plot showing the relationship between clast mass and dimensional values; C) Frequency of clasts classified by sphericity and roundness; and D) Plasticlast shapes plotted on a Zingg (1935) diagram.

Raman spectra obtained from different regions of all collected plasticlasts, as exemplified in Figure 7, revealed that the polymeric matrix primarily consists of HDPE. The spectra displayed characteristic bands corresponding to phthalocyanine compounds, which are consistent with those observed in in-situ plastistone. Notably, in the greener samples, the intensity of the phthalocyanine peaks was significantly higher compared to

Preprint not peer reviewed

This preprint research paper has not been peer reviewed. Electronic copy available at: https://ssrn.com/abstract=5372354

the grayish samples, where these intensity peaks were almost imperceptible in some cases (Figure 7).

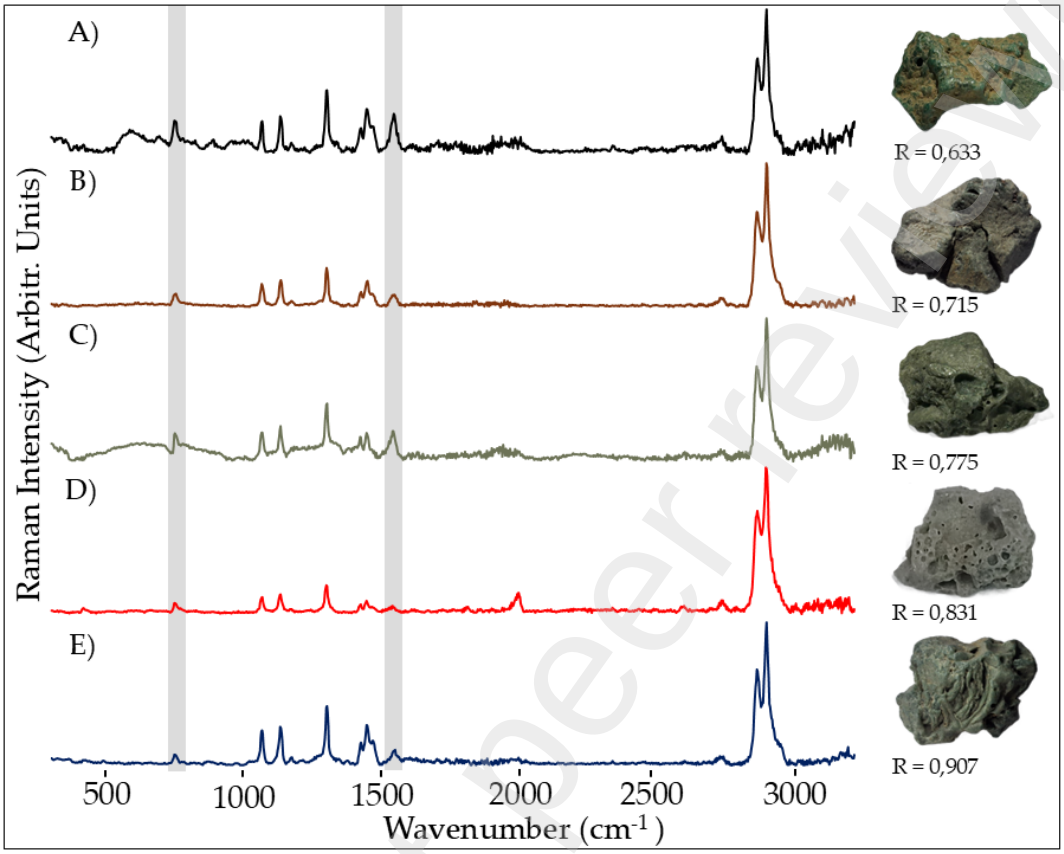


Figure 7: Raman spectra (A–E) on the left show varying intensity at dye-related peaks marked by gray bands. On the right are the matching plasticlasts, with colors from dark green to gray and varying roundness (R) values from ImageJ.

4. OUTLOOK

Anthropogenic stones are widespread issue found on multiple beaches of Trindade Island, the most remote island with such pollution reported. Their presence results mainly from erosion and transport of in-situ plastistone monitored over five years. Composed of HDPE with phthalocyanine green dyes, they derive from green maritime ropes. Our study is pioneering in using portable Raman spectroscopy as a baseline to identify polymer

Preprint not peer reviewed

This preprint research paper has not been peer reviewed. Electronic copy available at: https://ssrn.com/abstract=5372354

types and other additives in melted plastic matrix and track the source of plastic items. This approach is useful for direct field analysis in proposing monitoring plastic pollution in beaches.

PE is ubiquitous in ocean plastic pollution (e.g., Geyer, 2020; Rochman, 2013), including novel plastic debris forms (e.g., Shruti et al., 2023), and dyes additives present in manufacturing plastics in a concerning (e.g., Caggiani et al., 202; Espiritu et al. 2023, Key et al., 2024), since they affect the rate of environmental degradation and the evolution of plastic debris (Key et al., 2024). Pollution from shipping and maritime activities has a significant impact on microplastic formation worldwide (e.g., Napper et al., 2022; Welden and Cowie, 2017; da Rocha et al., 2021). Additionally, ropes litter are susceptible to forming novel plastic debris forms under natural conditions, as evidenced by Ehlers et al. (2021).

Field monitoring and morphometric analysis of clasts (shape, roundness, sphericity) are key to understanding transport and reworking over time in complex depositional context (e.g., McLaren & Bowles, 1985; Bui et al., 1989; Attal & Lavé, 2009; Lukas et al., 2013; Allen, 2017; Auel et al., 2017). Plasticlasts with low sphericity suggest moderate, short-range transport, while subrounded, high-sphericity ones indicate prolonged transport and abrasion.

During transportation and deposition in a marine environment (e.g., de Souza et al., 2012; Lessa et al., 2000; McCave, 1984; Ramalho, 2013), plastic materials likely degrade more readily than volcanic rocks, which accounts for the observed morphometry of the transported materials. Furthermore, anthropogenic stones complexes act as hotspots for microplastic generation, although they tend to fragment less readily than typical plastic debris (Wang et al., 2023).

Preprint not peer reviewed

This preprint research paper has not been peer reviewed. Electronic copy available at: https://ssrn.com/abstract=5372354

Plasticlasts collected at Tartarugas Beach were found in expressive concentrations along the shoreline and buried within turtle nests. As these buoyant fragments are easily transported by currents and storms (e.g., de Vries et al., 2020), their presence indicates marine-driven dispersion. Our results also show that turtle nests function as natural traps for plastistones, whose composition and additives highlight a concerning marine pollution scenario.

In this sense, anthropogenic stones illustrate troubling scenario relation to marine pollution, demonstrating the persistence of green PE maritime ropes to melting, transport, and burial processes. These factors make them strong candidates to represent marine debris preserved in Earth's strata.

DECLARATION OF GENERATIVE AI AND AI-ASSISTED TECHNOLOGIES IN THE WRITING PROCESS

During the preparation of this work the authors used Chat-GPT and Apple Intelligence tool to improve language and readability, with caution. After using this tool/service, the authors reviewed and edited the content as needed and took full responsibility for the original content of this publication.

ACKNOWLEDGEMENTS

We thank LECOST/UFPR, the Brazilian Navy, CNPq, and CIRM for financial support (project 443254/2019-2). This work was also supported by FAPESP (grants 2023/10087-8 and 2018/22214-6), CNPq (306501/2022-8, 311837/2022-0, 314836/2023-3), and INCT/INEO (2014/50869-6 and 465572/2014-6).

Preprint not peer reviewed

This preprint research paper has not been peer reviewed. Electronic copy available at: https://ssrn.com/abstract=5372354

REFERENCES

Allen, P. A., 2017. Sediment routing systems: The fate of sediment from source to sink. Cambridge University Press.

Angelin, E. M., França de Sá, S., Picollo, M., Nevin, A., Callapez, M. E., Melo, M. J., 2021. The identification of synthetic organic red pigments in historical plastics: Developing an in situ analytical protocol based on Raman microscopy. Journal of Raman Spectroscopy. 52(1), 145-158. https://doi.org/10.1002/jrs.5985.

Angulo, R. J., de Souza, M. C., Barboza, E. G., da Camara Rosa, M. L. C., Fernandes, L. A., Guedes, C. C. F., de Oliveira, L.H.S, Manzolli, R.P., Disaró, S.T., Ferreira, A.G., Martin, C. M., 2018. Quaternary sealevel changes and coastal evolution of the Island of Trindade, Brazil Journal of South American Earth Sciences. 84, 208-222. https://doi.org/10.1016/j.jsames.2018.04.003.

Attal, M., Lavé, J., 2009. Pebble abrasion during fluvial transport: Experimental results and implications for the evolution of the sediment load along rivers. Journal of Geophysical Research: Earth Surface. 114, F4. https://doi.org/10.1029/2009JF001328.

Auel, C., Albayrak, I., Sumi, T., Boes, R. M., 2017. Sediment transport in high-speed flows over a fixed bed: 2. Particle impacts and abrasion prediction. Earth Surface Processes and Landforms. 42(9), 1384-1396. https://doi.org/10.1002/esp.4132.

Azari, A., Ronsmans, S., Vanoirbeek, J. A., Hoet, P. H., Ghosh, M., 2024. Challenges in Raman spectroscopy of (micro) Plastics: The interfering role of colourants. Environmental Pollution. 363, 125250. https://doi.org/10.1016/j.envpol.2024.125250.

Bui, E. N., Mazzullo, J. M., Wilding, L. P., 1989. Using quartz grain size and shape analysis to distinguish between aeolian and fluvial deposits in the Dallol Bosso of Niger

Preprint not peer reviewed

This preprint research paper has not been peer reviewed. Electronic copy available at: https://ssrn.com/abstract=5372354

(West Africa). Earth Surface Processes and Landforms. 14(2), 157-166. https://doi.org/10.1002/esp.3290140206.

Bratashov, D. N., Masic, A., Yashchenok, A. M., Bedard, M. F., Inozemtseva, O. A., Gorin, D. A., Basova, T., Sievers, T. K., Sukhorukov, G. B., Winterhalter, M., Möhwald, H., Skirtach, A. G., 2011. Raman imaging and photodegradation study of phthalocyanine containing microcapsules and coated particles. Journal of Raman Spectroscopy. 42(10), 1901–1907. https://doi.org/https://doi.org/10.1002/jrs.2938.

Caggiani, M. C., Cosentino, A., Mangone, A., 2016. Pigments Checker version 3.0, a handy set for conservation scientists: A free online Raman spectra database. Microchemical Journal. 129, 123–132. https://doi.org/10.1016/j.microc.2016.06.020.

Corcoran, P.L., Moore, C.J., Jazvac, K., 2014. An anthropogenic marker horizon in the future rock record. GSA Today. 24 (6), 4–8.

Corcoran, P. L., Jazvac, K., 2020. The consequence that is plastiglomerate. Nature Reviews Earth & Environment. 1(1), 6-7.

Cowger, W., Steinmetz, Z., Gray, A., Munno, K., Lynch, J., Hapich, H., Primpke, S., De Frond, H., Rochman, C., Herodotou, O., 2021. Microplastic spectral classification needs an open source community: open specy to the rescue! Anal. Chem. 93 (21), 7543–7548. https://doi.org/10.1021/acs.analchem.1c00123.

da Rocha, F. O. C., Martinez, S. T., Campos, V. P., da Rocha, G. O., de Andrade, J. B., 2021. Microplastic pollution in Southern Atlantic marine waters: review of current trends, sources, and perspectives. Science of the Total Environment. 782, 146541. https://doi.org/10.1016/j.scitotenv.2021.146541.

Preprint not peer reviewed

This preprint research paper has not been peer reviewed. Electronic copy available at: https://ssrn.com/abstract=5372354

de Souza, M. C., Angulo, R. J., Assine, M. L., de Castro, D. L., 2012. Sequence of facies at a Holocene storm-dominated regressive barrier at Praia de Leste, southern Brazil. Marine Geology. 291, 49-62. https://doi.org/10.1016/j.margeo.2011.10.009.

de Vries, S., Wengrove, M., Bosboom, J., 2020. Marine sediment transport. In Sandy Beach Morphodynamics. Elsevier. 187-212. https://doi.org/10.1016/B978-0-08-102927-5.00009-6.

Del Caño, T., Aroca, R., de Saja, J. A., Rodriguez-Mendez, M. L., 2003. Langmuir−Blodgett Mixed Films of Titanyl (IV) Pthalocyanine and Arachidic Acid. Molecular Orientation and Film Structure. Langmuir. 19(9), 3747–3751. https://doi.org/10.1021/la020825h.

Ehlers, S. M., Ellrich, J. A., Gestoso, I., 2021. Plasticrusts derive from maritime ropes scouring across raspy rocks. Marine Pollution Bulletin. 172, 112841. https://doi.org/10.1016/j.marpolbul.2021.112841.

Espiritu, E. Q., Rodolfo, R. S., Evangelista, S. M. J., Feliciano, J. J. G., Sumaway, A. M. N., Pauco, J. L. R., Alvarez, K. V. N., Enriquez, E. P., 2023. Microplastics contamination in the fishes of selected sites in Pasig River and Marikina River in the Philippines. Marine Pollution Bulletin. 187, 114573. https://doi.org/10.1016/j.marpolbul.2023.114573.

Fernandino, G., Elliff, C. I., Francischini, H., Dentzien-Dias, P., 2020. Anthropoquinas: first description of plastics and other man-made materials in recently formed coastal sedimentary rocks in the southern hemisphere. Marine Pollution Bulletin. 154, 111044.

Fernandino, G., Vidal, C., Ritter, M. D. N., Santos, F. A., 2025. Evidence of plastics integrating the geological cycle: plastic forms in coastal ecosystems along the southern Brazilian shoreline. Ocean and Coastal Research. 73, e25003. http://doi.org/10.1590/2675-2824073.23186.

Preprint not peer reviewed

This preprint research paper has not been peer reviewed. Electronic copy available at: https://ssrn.com/abstract=5372354

Gaffo, L., Constantino, C. J. L., Moreira, W. C., Aroca, R. F., Oliveira, O. N., 2002a. Atomic Force Microscopy and Micro-Raman Imaging of Mixed Langmuir−Blodgett Films of Ytterbium Bisphthalocyanine and Stearic Acid. Langmuir. 18(9), 3561–3566. https://doi.org/10.1021/la011234e.

Gaffo, L., Constantino, C. J. L., Moreira, W. C., Aroca, R. F., Oliveira, O. N., 2002b. Vibrational spectra and surface-enhanced resonance Raman scattering of palladium phthalocyanine evaporated films. Journal of Raman Spectroscopy. 33(10), 833–837. https://doi.org/10.1002/jrs.924.

Gaffo, L., Constantino, C. J. L., Moreira, W. C., Aroca, R. F., Oliveira, O. N., 2004. Surface-enhanced Raman scattering and micro-Raman imaging of Langmuir–Blodgett films of rhodium phthalocyanine. Spectrochimica Acta Part A: Molecular and Biomolecular Spectroscopy. 60(1–2), 321–327. https://doi.org/10.1016/S1386-1425(03)00229-4

Geyer, R., 2020, Production, use, and fate of synthetic polymers. In Plastic Waste and Recycling. 2, 13-32. https://doi.org/10.1016/B978-0-12-817880-5.00002-5.

Goswami, P., Bhadury, P., 2023. First record of an Anthropocene marker plastiglomerate in Andaman Island, India. Marine Pollution Bulletin. 190, 114802. https://doi.org/10.1016/j.marpolbul.2023.114802.

Key, S., Ryan, P. G., Gabbott, S. E., Allen, J., Abbott, A. P., 2024. Influence of colourants on environmental degradation of plastic litter. Environmental Pollution. 347, 123701. https://doi.org/10.1016/j.envpol.2024.123701.

Lessa, G. C., Angulo, R. J., Giannini, P. C., Araújo, A. D., 2000. Stratigraphy and Holocene evolution of a regressive barrier in south Brazil. Marine Geology. 165(1-4), 87-108. https://doi.org/10.1016/S0025-3227(99)00130-9.

Preprint not peer reviewed

This preprint research paper has not been peer reviewed. Electronic copy available at: https://ssrn.com/abstract=5372354

344 Liu, Y., Hu, J., Lin, L., Yang, B., Huang, M., Chang, M., Huang, X., Dai, Z., Sun, S.,
345 Ren, L., Li, C., 2023. Overcoming the fluorescent interference during Raman
346 spectroscopy detection of microplastics. Science of The Total Environment. 897, 165333.
347 https://doi.org/10.1016/j.scitotenv.2023.165333.

348 Lukas, S., Benn, D. I., Boston, C. M., Brook, M., Coray, S., Evans, D. J., Graf, A.,
349 Kellerer-Pirklbauer, A., Kirkbride, M.P., Krabbendam, M., Lovell, H., Machiedo, M.,
350 Mills, S.C., Nye, K., Reinardy, B.T.I., Ross, F.H., Signer, M., 2013. Clast shape analysis
351 and clast transport paths in glacial environments: A critical review of methods and the
352 role of lithology. Earth-Science Reviews. 121, 96-116.
353 https://doi.org/10.1016/j.earscirev.2013.02.005

354 McCave, I. N., 1984. Erosion, transport and deposition of fine-grained marine sediments.
355 Geological Society, London, Special Publications. 15(1), 35-69.
356 https://doi.org/10.1144/GSL.SP.1984.015.01.03.

357 McLaren, P., Bowles, D., 1985. The effects of sediment transport on grain-size
358 distributions. Journal of Sedimentary Research. 55(4), 457-470.
359 https://doi.org/10.1306/212F86FC-2B24-11D7-8648000102C1865D.

360 Napper, I. E., Wright, L. S., Barrett, A. C., Parker-Jurd, F. N., Thompson, R. C., 2022.
361 Potential microplastic release from the maritime industry: Abrasion of rope. Science of
362 The Total Environment. 804, 150155. https://doi.org/10.1016/j.scitotenv.2021.150155.

363 Nava, V., Frezzotti, M. L., Leoni, B., 2021. Raman spectroscopy for the analysis of
364 microplastics in aquatic systems. Applied Spectroscopy. 75(11), 1341-1357.
365 https://doi.org/10.1177/0003702821104431.

Preprint not peer reviewed

This preprint research paper has not been peer reviewed. Electronic copy available at: https://ssrn.com/abstract=5372354

366 Pigeon, M., Prud'homme, R. E., Pezolet, M., 1991b. Characterization of molecular
367 orientation in polyethylene by Raman spectroscopy. Macromolecules. 24(20), 5687–
368 5694. https://doi.org/10.1021/ma00020a032.

369 Ramalho, R. S., Quartau, R., Trenhaile, A. S., Mitchell, N. C., Woodroffe, C. D., Ávila,
370 S. P., 2013. Coastal evolution on volcanic oceanic islands: A complex interplay between
371 volcanism, erosion, sedimentation, sea-level change and biogenic production. Earth-
372 Science Reviews. 127, 140-170. https://doi.org/10.1016/j.earscirev.2013.10.007.

373 Rangel-Buitrago, N., Neal, W. J., 2023. A geological perspective of plastic pollution.
374 Science of the Total Environment. 893, 164867.
375 https://doi.org/10.1016/j.scitotenv.2023.164867.

376 Rangel-Buitrago, N., Ochoa, F. L., Rodríguez, R. D. B., Moreno, J. B., Trilleras, J.,
377 Arana, V. A., & Neal, W. J. (2023). Decoding plastic pollution in the geological record:
378 A baseline study on the Caribbean Coast of Colombia, north South America. Marine
379 Pollution Bulletin, 192, 114993.

380 Rochman, C.M., 2013. Plastics and priority pollutants: a multiple stressor in aquatic
381 habitats. Environ. Sci. Technol. 2439-2440.

382 Ryan, P. G., 2014. Litter survey detects the South Atlantic 'garbage patch'. Marine
383 Pollution Bulletin. 79(1-2), 220-224. https://doi.org/10.1016/j.marpolbul.2013.12.010.

384 Santos, F.A., Diório, G.R., Guedes, C.C.F., et al., 2022. Plastic debris forms: Rock
385 analogues emerging from marine pollution. Mar. Pollut. Bull. 182, 114031.

386 Saron, C., Felisberti, M. I., 2006. Influence of colorants on the degradation and
387 stabilization of polymers. Química Nova. 29, 124-128. https://doi.org/10.1590/S0100-
388 40422006000100022.

Preprint not peer reviewed

This preprint research paper has not been peer reviewed. Electronic copy available at: https://ssrn.com/abstract=5372354

Sato, H., Shimoyama, M., Kamiya, T., Amari, T., Šašic, S., Ninomiya, T., Siesler, H. W., Ozaki, Y., 2002a. Raman spectra of high-density, low-density, and linear low-density polyethylene pellets and prediction of their physical properties by multivariate data analysis. Journal of Applied Polymer Science. 86(2), 443–448. https://doi.org/10.1002/app.10999.

Sato, H., Shimoyama, M., Kamiya, T., Amari, T., Šašic, S., Ninomiya, T., Siesler, H. W., Ozaki, Y., 2002b. Raman spectra of high-density, low-density, and linear low-density polyethylene pellets and prediction of their physical properties by multivariate data analysis. Journal of Applied Polymer Science. 86(2), 443–448. https://doi.org/10.1002/app.10999.

Scherrer, N. C., Stefan, Z., Francoise, D., Annette, F., Renate, K., 2009. Synthetic organic pigments of the 20th and 21st century relevant to artist's paints: Raman spectra reference collection. Spectrochimica Acta Part A: Molecular and Biomolecular Spectroscopy. 73(3), 505–524. https://doi.org/https://doi.org/10.1016/j.saa.2008.11.029.

Shruti, V. C., Kutralam-Muniasamy, G., Pérez-Guevara, F., 2023. New forms of particulate plastics in the anthropocene. Earth-Science Reviews. 104601. https://doi.org/10.1016/j.earscirev.2023.104601.

Silva, D. J. da, Wiebeck, H., 2019. Predicting LDPE/HDPE blend composition by CARS-PLS regression and confocal Raman spectroscopy. Polímeros. 29(1). https://doi.org/10.1590/0104-1428.00218.

Turner, A., Wallerstein, C., Arnold, R., Webb, D., 2019. Marine pollution from pyroplastics. Sci.Total Environ. 694, 133610.

Waldschläger, K., Brückner, M. Z., Almroth, B. C., Hackney, C. R., Adyel, T. M., Alimi, O. S., Belontz, S.L., Cowger, W., Doyle, D., Gray, A., Kane, I., Kooi, M., Kramer, M.,

Preprint not peer reviewed

This preprint research paper has not been peer reviewed. Electronic copy available at: https://ssrn.com/abstract=5372354

Lechthaler, S., Michie, L., Nordam, T., Pohl, F., Russell, C., Thit, A., Umar, W., Valero, D., Varrani, A., Warrier, A.K., Woodall, L.C., Wu, N., 2022. Learning from natural sediments to tackle microplastics challenges: A multidisciplinary perspective. Earth-Science Reviews. 228, 104021. https://doi.org/10.1016/j.earscirev.2022.104021.

Wang, L., Bank, M. S., Rinklebe, J., Hou, D., 2023. Plastic–rock complexes as hotspots for microplastic generation. Environmental science & technology. 57(17), 7009-7017.

Welden, N. A., Cowie, P. R. 2017. Degradation of common polymer ropes in a sublittoral marine environment. Marine Pollution Bulletin. 118(1-2), 248-253. https://doi.org/10.1016/j.marpolbul.2017.02.072.

Wool, R. P., Bretzlaff, R. S., Li, B. Y., Wang, C. H., Boyd, R. H., 1986. Infrared and raman spectroscopy of stressed polyethylene. Journal of Polymer Science Part B: Polymer Physics. 24(5), 1039–1066. https://doi.org/10.1002/polb.1986.090240508.

Zalasiewicz, J., Waters, C.N., Ivar do Sul, J.A., Corcoran, P.L., Barnosky, A.D., Cearreta, A., Edgeworth, M., Gałuszka, A., Jeandel, C., Leinfelder, R., McNeill, J.R., Steffen, W., Summerhayes, C., Wagreich, M., Williams, M., Wolfe, A.P., Yonan, Y., 2016. The geological cycle of plastics and their use as a stratigraphic indicator of the Anthropocene. Anthropocene. 13, 4–17. https://doi.org/10.1016/j.ancene.2016.01.002.

Zingg, T. H., 1935. Beitrag zur Schotteranalyse: Schwiz. Min. u. Pet. Mitt.15, 39-140.

Zucolotto, V., Ferreira, M., Cordeiro, M. R., Constantino, C. J. L., Balogh, D. T., Zanatta, A. R., Moreira, W. C., Oliveira, O. N., 2003. Unusual Interactions Binding Iron Tetrasulfonated Phthalocyanine and Poly (allylamine hydrochloride) in Layer-by-Layer Films. The Journal of Physical Chemistry B. 107(16), 3733–3737. https://doi.org/10.1021/jp027573d.

Preprint not peer reviewed

This preprint research paper has not been peer reviewed. Electronic copy available at: https://ssrn.com/abstract=5372354